AIAA Paper 2012-0398, 50th AIAA Aerospace Sciences Meeting,
9-12 Jan. 2012, Nashville, TN, USA

# Towards High Efficiency Hypersonic Flight – Hypersonic Bi-Directional Flying Wing

Andy Nieto[*] , Karen Perez[*] , Marcus Rojas[*] , Omar Rodriguez[*] , Oscar Fernandez[*] , Skyler Salman[*] ,
GeCheng Zha[†]
*University of Miami*
*Department of Mechanical and Aerospace Engineering*
*Coral Gables, Florida, 33124*

## Abstract

**This paper examines the use of a hypersonic bi-directional flying wing concept for use in a high efficiency hypersonic system. The bi-directional flying wing concept consists of a symmetric planform which enables flight to occur at two different geometric configurations. The subsonic configuration would have a high aspect ratio and a low sweep. The aircraft would then rotate 90 degrees and enter the hypersonic configuration which would have a low aspect ratio and high sweep. This design overcomes the inherent conflict between subsonic and hypersonic flight in conventional hypersonic systems. The design was found to have high aerodynamic efficiency at both hypersonic and subsonic speeds. This concept could be applied to civil transports and military vehicles alike as the subsonic mode allows the aircraft to be operated on conventional runways. This paper examines some of the unique challenges that would be present in a hypersonic civil transport because of the need to ensure passenger comfort and safety. Optimization of the design is dependent on high speed multi-mode engines and high temperature resistant materials.**

## I. Introduction

This paper examines the design of a high efficiency hypersonic vehicles using the bidirectional flying wing concept first employed by Zha[1,2,3,4,5] for use in a supersonic vehicle. This concept successfully allows for many technical challenges involved in supersonic flight to be overcome. Many of the technical challenges involved in supersonic flight are also present in hypersonic flight; however some of these challenges become even greater, in addition to the new phenomena present at hypersonic speeds.

Hypersonic flight is defined as flight at or above Mach 5. At such high speeds, the temperatures experienced become extremely high. The temperatures often exceed the dissociation temperature of the molecules in the air, thus causing the flow to be a chemically reactive non-equilibrium flow[6,7]. The chemical reactions in the flow can have corrosive effects on the surface of the vehicle. At hypersonic speeds, the shock waves are very strong and the density of the air behind the shock increases substantially. This means that the volume behind the shock wave decreases substantially and as a result

[*] Senior Undergraduate Student

[†] Ph.D., Associate Professor, Director of Aerodynamics and CFD Lab

the shock waves are very close to the surface of the body. The fact that the shock waves are very close to the surface of the body and that these shock waves are very thin leads to viscid – inviscid interactions between the boundary layer and the shock layer which is of the same magnitude as the boundary layer.

Currently there are no hypersonic or even supersonic civil transports in service. The only supersonic transports flown were the Tipolev Tu-144 and the Concorde. The Tupolev was retired in 1978, while the Concorde was retired in 2003. While there have been successful supersonic vehicles, mostly for military use, hypersonic vehicles for either military or civilian purposes are only in the early stages. Hypersonic vehicles have been used successfully, however, in the form of spacecraft such as the space shuttles and the Apollo Program orbiters. Spacecraft typically overcome some of the hypersonic technical challenges by employing blunt body shapes in order to greatly reduce the surface heating. Orbiters such as those used in the Apollo Program were designed for relatively small lifespans, meaning that they were not meant to be reusable beyond their mission. This meant they would experience hypersonic flow conditions only during escape from and entry into Earth's atmosphere. Ablative materials were used in order to withstand the high temperatures, however the use of ablative materials such as PICA[8] are not practical for use in reusable vehicles such as civil transport and military aircraft.

A more recent hypersonic vehicle is the Boeing X-51, which was part of the X-51 Waverider program and achieved flight speeds up to Mach 6. This vehicle was used to show the advantages of using a waverider concept, which has been shown to have high lift to drag ratios on computational studies[9]. The high aerodynamic efficiency is obtained by basing the design on a known supersonic flow field in order to capture a bow shock along the leading edges on the pressure surface. This reduces the spillage of flow and thus retains more of the high pressured flow in the pressure surface.

Another successful hypersonic demonstrator was the NASA X-43A which is part of NASA's Hyper-X Program[10,11]. The X-43A is the first vehicle to fly at hypersonic speeds by using an air breathing engine. A SCRAMJET engine was used to successfully propel the vehicle to speeds of Mach 7 and Mach 10. Both the X-43and X-51 are optimized for hypersonic flight and are not design for subsonic flight. Neither of these aircraft is able to take-off on its own; instead both these aircraft are brought in altitude by a large transport such as a B-52. The B-52 brings the hypersonic vehicle to a speed where the SCRAMJET engines will work and then the vehicle is detached from the B-52.

Currently Reaction Engines Limited is working on two hypersonic vehicles which would be able to take-off and land on conventional runways[12,13,14,15]. The LAPCAT A2, which is partially funded by the European Union, is designed to be a hypersonic civil transport that would use multi-mode air breathing engines. The proposed engine is the conceptual Scimitar Engine which operates in a turbo-fan configuration during subsonic flight, and switches into a ramjet mode during supersonic and hypersonic (Mach 5) flight. The other proposed hypersonic vehicle from Reaction Engines Limited is the Skylon, which is designed to be a single stage to orbit (SSTO) unmanned space plane. Skylon would use Reactions Engines conceptual SABRE engine which is a multi-mode engine which can operate in orbit. The SABRE engine would operate as a ramjet while in the atmosphere, and then switch into a rocket engine mode once orbit was reached.

The disadvantage of the Reaction Engines Limited concepts are that even though the engines have multiple modes, the actual geometry of the aircraft will only have one mode. There have been no hypersonic designs that employ variable geometries; however variable geometries have been used successfully in supersonic aircrafts. The oblique flying wing[16,17] concept not only provides multiple geometries but it also eliminates the fuselage which is not a significant source of lift. The sweep angle of this concept can be changed while in flight, thus allowing it to fly with a low swept wing and high aspect

ratio during subsonic flight, and then switch to a high swept wing with a low aspect ratio during supersonic flight. The disadvantage to the oblique flying wing concept is that asymmetry of the design which leads to instabilities during flight[18,19], this would mean the design would need complex and expensive control surfaces and systems. The size of an oblique flying wing would also be very large for a civil transport as the airfoil thickness must be thick enough to accommodate passengers.

## II. Hypersonic Bi-Directional Flying Wing Concept

The proposed concept would employ different geometrical configurations in order to attain high efficiency flight at subsonic, supersonic, and hypersonic speeds. The aircraft would be a flying wing with a symmetric planform about both the longitudinal and span axes.

The subsonic configuration would consist of a low swept design with a high aspect ratio as can be seen in Fig. 1(aspect ratio is 5.80 and sweep is 20 degrees.) The airfoil of the subsonic configuration is thicker than that for the hypersonic configuration, as a thick airfoil is needed to achieve the high lift coefficient needed for subsonic flight. The subsonic configuration would allow the aircraft to have efficient flight at subsonic speeds which is necessary for take-off and landing. The subsonic configuration enables the aircraft to use conventional runways for take-off and landing.

Before transitioning to supersonic flight, the aircraft would rotate 90 degrees along its axis in order to attain the hypersonic configuration which is shown in Fig. 2 (aspect ratio is 1.45 and sweep is 70 degrees.) This rotation would cause the sweep angle to increase and the aspect ratio to decrease; both these features are highly desirable for supersonic and hypersonic flight. The airfoil for the hypersonic configuration is much thinner than the subsonic airfoil and features a wedge shaped leading edge in order to reduce the high drag forces that will be encountered during hypersonic flight.

This concept eliminates the inherent conflict between subsonic and supersonic performance which is present in conventional supersonic/hypersonic concepts which only have one geometrical configuration. The symmetry of the design also eliminates the possibility of having difficulties with stability and controls systems. The design also features a flat pressure surface in order to minimize the strong sonic boom effects during hypersonic flight.

The initial design tested a had a relatively low sweep in the hypersonic configuration, although still substantially higher than that of the subsonic configuration. The initial design is shown in Fig. 3, and although it had a low aspect ratio, it did not have a high aerodynamic efficiency. The second design explored had a much higher sweep in the hypersonic configuration, while maintaining the round edges needed to avoid extremely high surface heating. The increased sweep would provide more 3-D wing effects, which means that the effective Mach number at the tips of the wing is significantly lower than that at the middle of the wing[20].

## III. Computational Fluid Dynamics (CFD) Analysis

The in house FASIP (Flow-Acoustics-Structural Interaction Package) CFD code is used for the simulations. FASIP has been intensively validated for various 2D and 3D steady and unsteady flows. FASIP has implemented advanced numerical algorithms including various approximate Riemann

solvers[21,22,23], 3rd order MUSCL schemes, high order WENO schemes and central differencing schemes[24,25,26,27], non-reflective boundary conditions[28], implicit unfactored Gauss-Seidel dual time stepping for unsteady calculation[29,30], fluid-structural interaction[31,32,33], Reynolds averaged Navier-Stokes turbulence models[34,35], DES and LES[36,37,38,39], preconditioning for incompressible flows[40,27], and high scalability parallel computing[41]. For the sonic boom calculation in this paper, the Roe's approximate Riemann solver[42] with 3rd order MUSCL scheme[43] and Minmod limiter is used.

The meshes used for both the subsonic and hypersonic simulations were H-Type meshes. For the hypersonic simulation the mesh was inclined by 30 degrees in order to better capture the shocks. The entire mesh used for the hypersonic simulations is shown in Fig. 5. The wing body used in the hypersonic simulation is shown in Fig.6. Only half of the aircraft needs to be simulated since the aircraft is symmetric along the flow direction. The same wing body is used for the subsonic except that it is rotated 90 degrees and the symmetry interface occurs along the chord of the subsonic airfoil.

### A. CFD Assumptions

The computational fluid dynamics simulations were done only on the wing body, meaning that all results presented in this paper do not include the effects of the engine. For both the subsonic and hypersonic simulations the flow calculations were done using Reynolds Average Navier Stokes (RANS) equations with viscous terms included. The hypersonic simulations were done under the assumption that the flow is in equilibrium, which means the molecules in the air are assumed not to dissociate and become reactive. Also, the hypersonic simulations are done without taking into consideration the viscid – inviscid interactions between the thin shock layer and the boundary layer that would occur at the leading edges of the aircraft.

### B. Hypersonic Simulation Results

The results of the simulations for the first design are shown in Fig. 7, where the lift and drag coefficients are plotted against the angle of attack. While a negative lift coefficient is expected at an angle of attack of zero because of the strong shock waves, it is still desirable to obtain higher lift coefficients and lower drag coefficients. The moment coefficient was positive at an angle of attack of zero, as can be seen in Fig. 8, this is a necessary criteria for stability. Fig.9 shows the Mach contours of the first design at the center of the wing body. These contours along with the contours shown in Fig. 10 are both at an angle of attack of zero. It can be seen in Fig. 10 that the characteristics of the flow do not change much throughout the span of the wing. In both the center slice and the wing tip slice a strong shock wave is observed at the leading edge, and in the trailing edge there is a strong expansion wave.

The Mach contours of the first design at an angle of attack of 5 degrees are shown in Fig. 11 and Fig. 12. It can be seen that at higher angles of attack the expansion waves at the trailing edge become stronger and the intensity remains constant throughout the wing span. The expansion waves are so strong because the trailing side of the aircraft effectively acts as a supersonic diffuser.

The second design featured a more highly swept design and the results are shown in Fig. 13 and Fig. 14. This design had higher lift coefficients and lower drag coefficients than the initial design. The aerodynamics continued to increase as the angle of attack was increased and the moment coefficient decreased as the angle of attack increased. These are both favorable trends as hypersonic flight would take place at a high angle of attack. The Mach contours of the second design at an angle of attack of zero

are shown in Fig. 15 and Fig. 16. At the center slice there is still the strong shock wave at the leading edge and a strong expansion wave in the trailing edge. However, at the wing tips, both the intensity of the shock wave and the expansion wave are greatly reduced. Fig. 17 and Fig. 18 show the Mach contours at an angle of attack of 5 degrees, and it can be observed that while there are strong shock and expansion waves at the center slice, at the wing tips the intensity of the shock and expansion waves are greatly reduced. This decrease in intensity is due to the higher sweep of the wing which causes the effective Mach number at the wing tips to be much lower than that of the leading center at the center of the wing body. This decrease in intensity of the shock and expansion waves at the wing tips is the reason why this design had higher lift coefficients and lower drag coefficients, which resulted in a higher aerodynamic efficiency than the initial design.

Another vital part of designing a hypersonic vehicle is to determine how high the surface heating will be. At a speed of Mach 8, the normalized free stream temperature is 13.8. The designated cruise altitude for the hypersonic vehicle was 90,000 ft, where the temperature is 224 Kelvin. The normalized temperature contours of the suction surface are shown in Fig. 19, and the normalized temperature contours of the pressure surface are shown in Fig. 20. It can be seen that on the suction surface the aircraft experiences normalized temperatures of up to 19.2. This indicates that the suction side of the aircraft will experience temperatures as high as 4300 Kelvin. It should also be kept in mind, that the temperatures on the pressure surface would actually be significantly on the trailing edge because of the engine exhaust which would be extremely high due to the tremendous amount of thrust required to cruise at Mach 8.

It was also desirable to demonstrate that this design could also fly efficiently at supersonic speeds. A simulation was done at Mach 3 and the results are shown in Fig. 21 and Fig. 22. It can be seen that at an angle of attack of zero, the lift coefficient is not negative as in the hypersonic case. The drag coefficient is also smaller throughout the range of angles of attack, this is likely due to the large decrease in wave drag. The lift coefficients at higher angles of attack are slightly less than in the hypersonic case. Overall, the aerodynamic efficiency at small angles of attack is much great in the supersonic case than in the hypersonic case. At higher angles of attack the aerodynamic efficiency is similar in both cases. The Mach contours are shown in Fig. 23 and Fig.22, and it can be seen that the Mach cone angle is much greater than in the hypersonic case, as would be expected. The high sweep still has the desired effect of decreasing the effective Mach number at the wing tip which decreases the intensity of shock and expansion waves.

### C. Subsonic Simulation Results

Simulations were also done for the subsonic case, where the aircraft would be rotated 90 degrees about the engine in order to obtain a configuration more favorable for subsonic flight. The results for the simulation done at Mach .85 are shown in Fig. 25 and Fig. 26. At low angles of attack, the aircraft is not very efficient, however this is not an issue, as the subsonic mode would be used mainly during take-off and landing where very high angles of attack are used. Two important observations are that the lift continues to increase as the angle of attack increases and there is no evidence of a stall value having been reached. Also, the moment coefficient decreases at higher angles of attack which is important as the aircraft would be flying at high angles of attack thus reducing stability concerns. The Mach contours at an angle of attack of zero are shown in Fig. 27, and the Mach contours at an angle of attack of eight are shown in Fig. 28. At an angle of attack of zero is can be seen that the Mach numbers spike up near the leading edges and the trailing edges. At an angle of attack it is evident that there is a normal shock at the trailing edge. This means that at Mach .85 the flow is actually transonic. Flight at transonic speeds is

typically inefficient because of the shock waves and it is therefore desirable to avoid flying at transonic speeds.

The next simulation was done at Mach .6 in order to avoid transonic flow, and the results are shown in Fig. 29 and Fig. 30. The performance improves significantly across all angles of attack. At an angle of attack of zero lift coefficient is positive, whereas in the transonic case it was negative. The aerodynamic efficiency (L/D) at higher angles of attack increases by as much as 2 and at least over 1. Flying at Mach .6 provides much higher aerodynamic efficiency and since it is used mostly for take-off and landing the decrease in speed is not a disadvantage. The Mach contours at an angle of attack of zero are shown in Fig. 31, and the Mach contours at an angle of attack of eight are shown in Fig. 32. While there are still some slight jumps in Mach number near the leading and trailing edges, they are no longer above Mach 1. It can also be seen that there is no longer a normal shock at an angle of attack of eight. The improvement is performance due to the absence of shock waves which indicates the flow regime is not transonic.

## IV. Design of Civil Transport

The design of a hypersonic civil transport is investigated in this paper in order to point out some of the major hurdles that need to be overcome before hypersonic flight is a reality. A civil transport is chosen as this is the case where the most obstacles appear as the safety and comfort of passengers is critical. Some of these obstacles would not be present in military or unmanned systems where there are no passengers or there comfort is not as essential. Our proposed civil transport would have a chord length of 40 m in the subsonic mode, and a chord length of 80 m in the hypersonic mode. This would correspond to a maximum thickness of 4 m.

### A. Engine Assumptions

Although this paper presents a solution to the inherent conflict between subsonic and hypersonic flight present in conventional hypersonic systems, it does not address the means in which subsonic and hypersonic flight is achieved. The hypersonic concept presented in this paper presents an wing that would fly efficiency at subsonic and hypersonic speeds, however currently there are no engines that can function at both subsonic and hypersonic speeds. In this section, some of the current conceptual engines being proposed for subsonic and hypersonic flight will be presented, along with the advantages and disadvantages they provide for a civil transport.

As, was previously stated, Reaction Engines Limited is working on a hypersonic civil transport that would employ the Scimitar which is in development and is shown in Fig. 33. This engine has a turbojet mode for subsonic flight and low supersonic flight, and then a ramjet for high supersonic speeds. The maximum speed this engine can function in is about Mach 5. Our hypersonic concept would cruise at Mach 8 and therefore this engine would not be adequate, however a similar concept would be needed. An engine like the scimitar would need to be expanded upon in order to include a configuration that allows it to function as a SCRAMJET engine capable of functioning at speeds of Mach 8. SCRAMJET engines are advantageous as they provide a means to achieve high velocities without the need for an onboard oxidizer.

The proposed Skylon space plane by Reaction Engines Limited would use the SABRE engine which is shown in Fig. 34. The Skylon space plane is designed to reach orbit and therefore it needs a rocket engine mode since there is no atmosphere for an air-breathing engine to work. Our hypersonic concept was intended to cruise at an altitude of 90,000 ft, and our simulations took the corresponding atmospheric conditions into account. However, the use of an engine with both ramjet and rocket modes would have some advantages despite the weight penalty caused by the need to carry liquid hydrogen and liquid oxygen on board. As was seen in the surface temperature analysis, the

surface temperatures experienced when flying at Mach 8 at an altitude of 90,000 feet would be very high. Using rocket engines would give two potential advantages, the liquid hydrogen and oxygen could be diverted throughout the aircraft near the outer surface and function as a heat exchanger, thus provided the foundation for a cooling system that would lower the surface temperatures. Also, using a rocket engine would mean that the aircraft could operate at much higher altitudes, if the aircraft were to function as a suborbital aircraft it could reach heights where the free stream temperature is much lower and thus the aircraft surface temperatures would also be significantly lower. It must be acknowledged that designing an aircraft designed to function at suborbital heights would provide additional challenges that would not be present when flying at 90,000 ft.

### B. Take-off and Landing

Take-off and landing would occur in the subsonic mode. Preliminary estimates for the takeoff and landing distances of our proposed hypersonic civil transport are 4354 ft and 3479 ft respectively. Both of these distances would allow the aircraft to use conventional runways in most of the major airports in the world. FAA regulations also require a pilot to have adequate visibility during take-off and landing which means the aircraft would have to have windows in the leading edge of the subsonic mode and the cockpit would have to be located here. Given technological technologies that are being developed for aviation systems, it is possible these regulations will one day change. Virtual pilot systems are being developed where the pilot can be aware and in full control of his surrounding through the use of external cameras, GPS, and other avionic systems. Large windows on a hypersonic civil transport would provide the technical challenge of making sure they can resist the high temperatures that are experienced during hypersonic flight.

### C. Transition Phase

Once the aircraft has taken off and has reached sufficient altitude, it will be time to transition into the hypersonic mode in order to cruise at hypersonic speeds. The transition must occur before the sonic barrier is reached as the subsonic mode is not suitable to withstand the strong shocks that occur as velocity increases past Mach 1. The transition would take place at an altitude of about 50,000 ft and at a speed of about Mach .7. The transition phase must thread a thin line between flight dynamics and passenger safety and comfort.

These factors also influence the mechanism which would be used to rotate the wing 90 degrees about the engine. The engine could be rotated purely by aerodynamic forces (yaw) by using ailerons or flaps. Alternatively, the engine could be rotated by a mechanism which is driven by a hydraulic system. The disadvantage of a driving mechanism is ensuing weight penalty caused by the hydraulic systems. However, with a driving mechanism, the rate of rotation would be able to be controlled very easily. This is a huge advantage as the aircraft cannot rotate so quickly that it causes passengers to experience large inertial forces.

Using flaps, it would be extremely difficult to control the rate of rotation. A quick rotation does have the advantage of not causing a large aerodynamic disturbance which means there would be little to no instabilities during transition. With a slower rotation, the plane would fly at a transitional phase for a longer period, and the planform would be non-symmetrical at this time which would lead to an uneven lift distribution and large instabilities. Additional flaps and ailerons would be needed to ensure stability during transition if the rotation will occur slowly. Further optimization would need to be done to ensure a design that is aerodynamically stable while at the same time rotating at a rate that does not cause discomfort to the passengers.

### D. Cabin Configuration

The location of the passenger cabin can aid in ensuring passenger comfort. When the aircraft is spinning, the inertial forces will be greatest at the extremities of the wings and therefore it is necessary to place passengers closer to the center of the aircraft where the inertial forces caused by the rotations will be smallest. The cabin floor layout is shown in Fig. 35, and the cabin floor plan is shown in Fig. 36. The floor plan is designed to seat approximately 185 passengers and crew members. The cabin would be split into four general areas, each having five rows, where each row has 8-10 seats. Each area has its own restroom facilities, which are closest to the center of the aircraft thus the restroom area will experience the smallest inertial forces.

This configuration is intended to be for a system where the aircraft rotates through the use of aerodynamic forces and not a driving mechanism. A driving mechanism would be located in the center of the aircraft and take up some of the space designated for passengers. Each seat has a width (includes space between seats) of .8 m, and .46 m of legroom. The aisles between the four sections that is used to provide food/beverage services is .75 m, and the cockpit is 4.68 m wide. The cockpit is located between two of the seating areas, the other space between seating areas is to be used for storage and baggage.

### E. Materials

As stated before, spacecraft that travel at hypersonic speeds during escape and entry employ ablative in order to withstand the extreme temperatures. Ablative materials would not be suitable for a reusable vehicle such a civil transport as material would have to be replaced frequently. As the CFD analysis showed, the highest surface temperatures exceed 4300 K. Currently the only material that could withstand these temperatures is Tantalum Hafnium Carbide which can resist temperatures up to 4488 K. This material is not currently available as a material for manufacturing, most likely because of its high density which would make it impractical for making bulk parts especially for an aircraft where low weight is so essential. Tantalum Hafnium carbide is available as part of a ceramic coating, however it can only resist temperatures up to 4163 K.

This means that there are not materials currently suitable to withstand the high surface temperatures without the use of a cooling system. Even with a cooling system, the temperatures would still be high and very few materials would be able to provide a sufficient safety margin and many of these materials, such as titanium and tungsten are very dense and expensive. To ensure adequate thermal protection as well as relatively low weight, a breakthrough in materials science is likely needed. The materials must also be malleable enough that they can be manufactured into the correct shapes, while still having very small tolerances. The thermal protection system of the aircraft would likely have a combination of light weight high temperatures alloys, heat resistant coatings, and an internal cooling system.

## V. Future Research

Further research is needed to gain a better grasp on what the maximum potential of the design is. From Fig. 13, Fig. 21, Fig. 25, and Fig. 29 it could be seen that an upper limit of aerodynamic efficiency had yet to be reached for subsonic, supersonic, and hypersonic performance. A stall value had clearly not been

reached so further simulations at higher angles of attack are needed to observe what the maximum possible aerodynamic efficiencies are. Simulations at other hypersonic speeds are also needed in order to see if the aircraft has an optimal speed for aerodynamic efficiency. Simulations at higher angles of attack for subsonic flight are of particular importance because the maximum lift coefficient heavily influences the take-off and landing distances. If higher lift coefficients are obtained the take-off and landing distances would become smaller.

Another important aspect of the design to analyze is the performance of the aircraft with the engine. Simulations of the design including the engine are critical to understanding the true potential of the design as the engines will be a significant source of drag. The fact that the engine is located on the bottom will also lead to large sonic boom effects propagating to the ground. Analysis of the sonic boom signature need to be done in order to better understand whether this aircraft would be able to fly over ground or whether its flight route would have to be constrained to the ocean and other unpopulated areas.

This paper investigated some of the obstacles that would be present in designing a hypersonic civil transport; however, implementation of this design would be much quicker in military applications especially unmanned drones or fighters. One of the big obstacles to designing a civil transport was the possible discomfort that passengers would experience during transition. Also a slow transition would lead to less inertial forces on passengers but there would be more instability. In an unmanned drone the transition phase could occur at rapid speeds and this means the flow would have little disturbance during transition and instabilities due to transition would be minimal or nonexistent. If the aircraft is shown to have even better aerodynamic performance at subsonic speeds, it is also possible that the aircraft could take-off from aircraft carriers making it a valuable military asset.

## VI. Conclusion

It is demonstrated that this concept has the ability to overcome the inherent conflict between subsonic and hypersonic performance found in conventional supersonic and hypersonic systems. The bidirectional wing concept provides a configuration with low sweep and a high aspect ratio for subsonic flight and a configuration with high sweep and low aspect ratio favorable for hypersonic flight. The ability to fly efficiently at subsonic speeds means the aircraft can take-off and land using conventional runways unlike current hypersonic vehicles which must be taken to the appropriate altitude and speed by a large transport. It is shown that the design has high aerodynamic efficiency at subsonic, supersonic, and hypersonic speeds. This concept would revolutionize both commercial civil transport and military systems. A civil transport that could cruise at Mach 8 would be able to travel between Miami and Shanghai in about four hours. Global travel between any two points in the world would be reduced to a matter of hours which would have many positive economic effects. Military vehicles that could travel at subsonic and hypersonic speeds efficiently would lead to drones and bombers that could take-off from aircraft carriers and reach their targets thousands of miles away in a matter of minutes not hours.

Optimization of this design is dependent on the availability of high speed multi-mode engines and high temperature resistant materials. The engines must have subsonic and hypersonic modes that correspond to the subsonic and hypersonic geometries of the aircraft. The high temperatures also require high temperature materials that are reusable, manufacturable, and light weight. Implementing the design for use in a civil transport would provide the additional challenges required to ensure passenger comfort and safety.

## Appendix

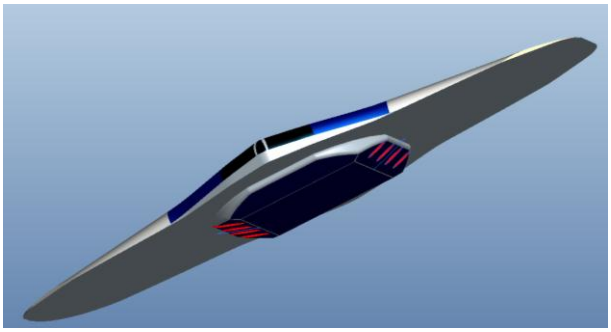

Figure1: Hypersonic Concept in Hypersonic Mode

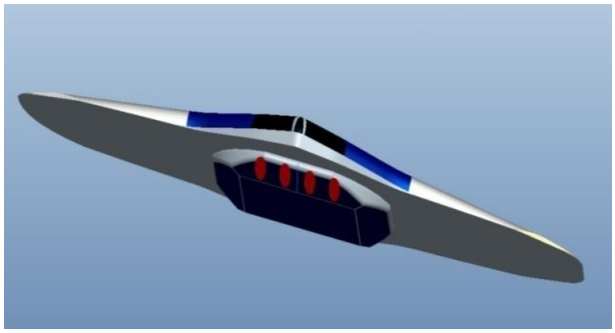

Figure 2: Hypersonic Concept in Subsonic Mode

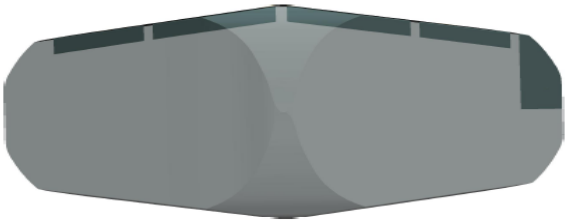

Figure 3: Low Sweep, Initial Design

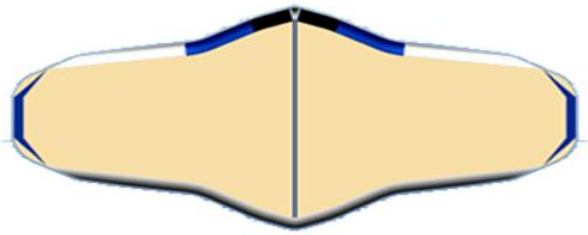

Figure 4: High Sweep, Current Design

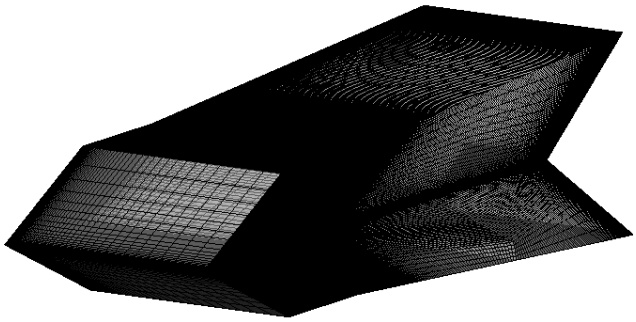

Figure 5: H-Type CFD Mesh

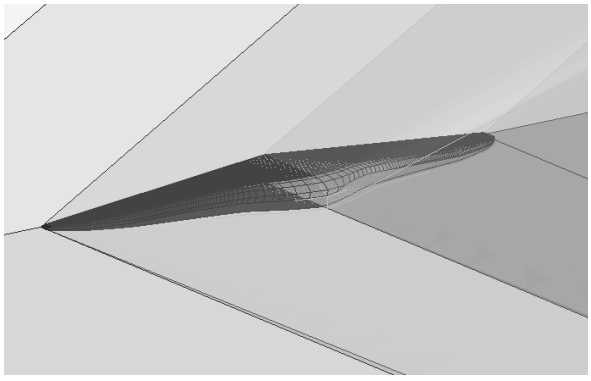

Figure 6: Wing Body CFD Mesh

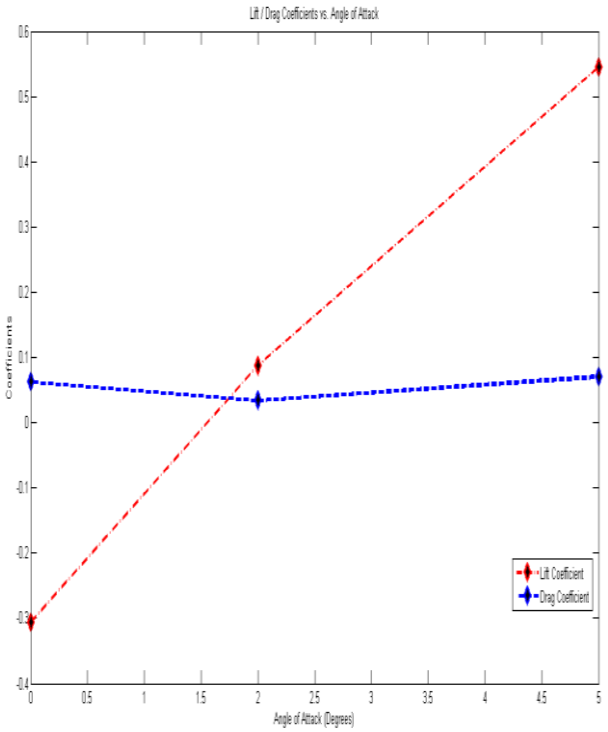


Figure 7: 1st Design, Lift and Drag Coefficients vs. AOA

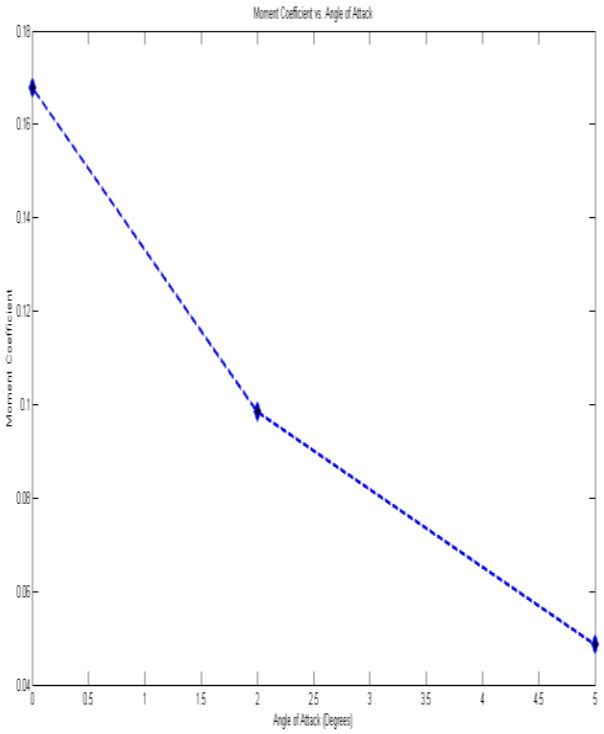


Figure 8: 1st Design, Moment Coefficient vs. AOA

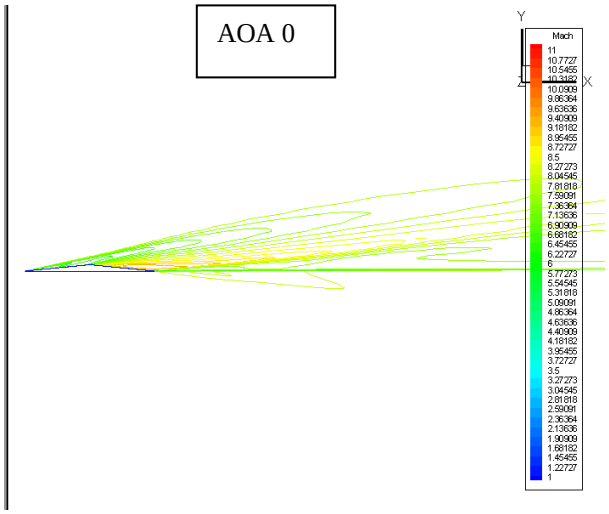


Figure 9: 1st Design, Center Slice Mach Contours

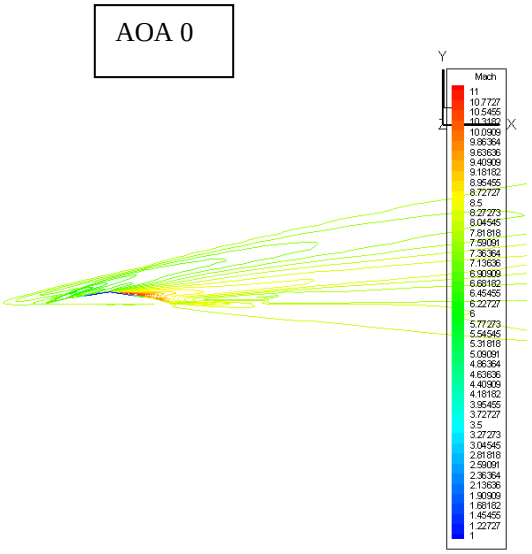


Figure 10: 1st Design, Wing Tip Mach Contours

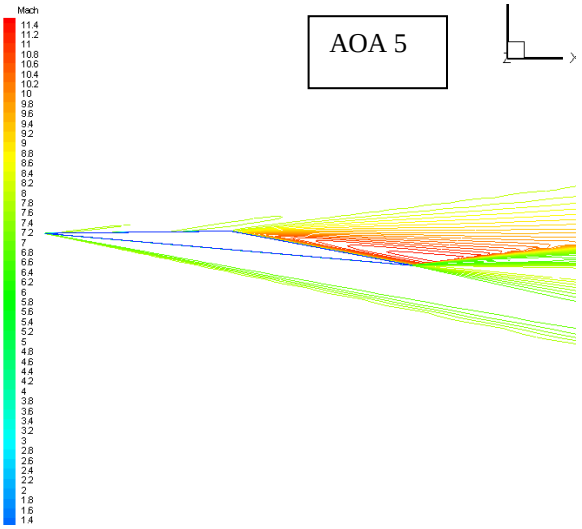


Figure 11: 1st Design, Center Slice Mach Contours

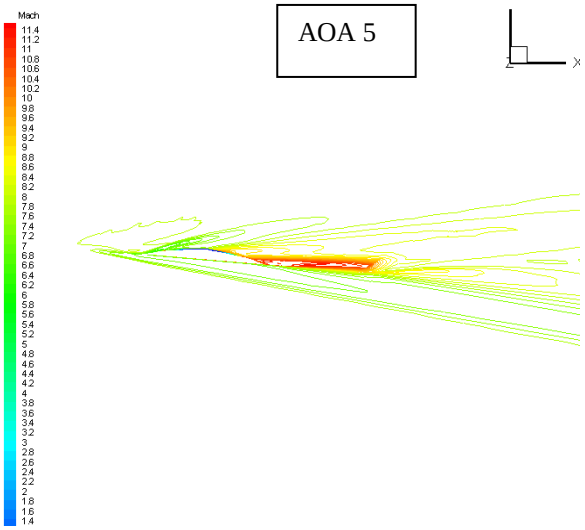


Figure 12: 1st Design, Wing Tip Mach Contours

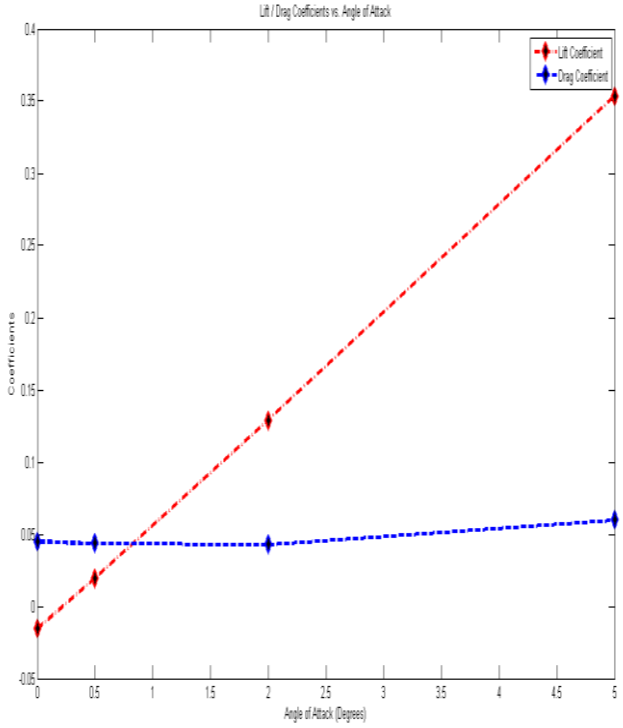


Figure 13:2nd Design, Lift and Drag Coefficient vs. AOA

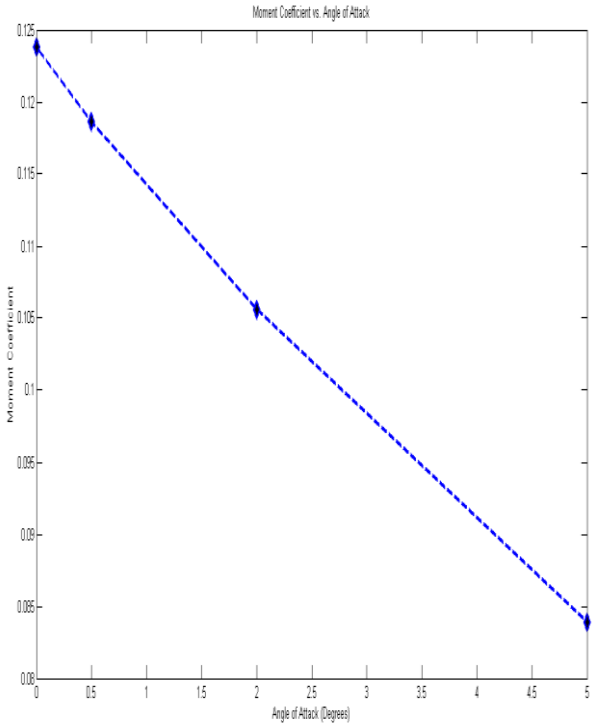


Figure 14: 2nd Design, Moment Coefficient vs. AOA

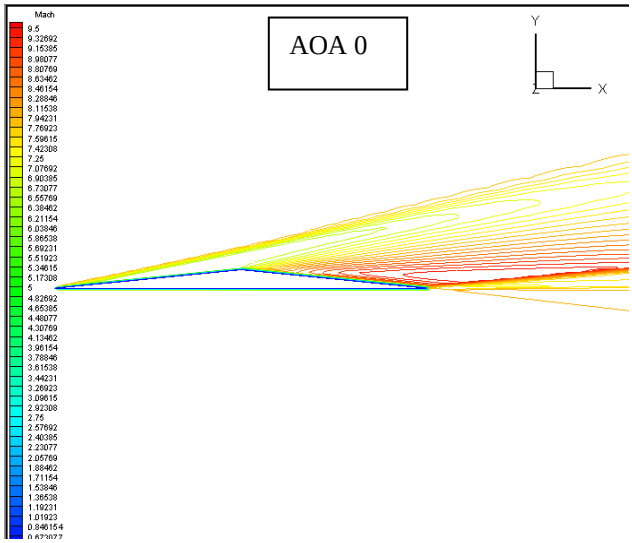


Figure 15: 2nd Design, Center Slice Mach Contours

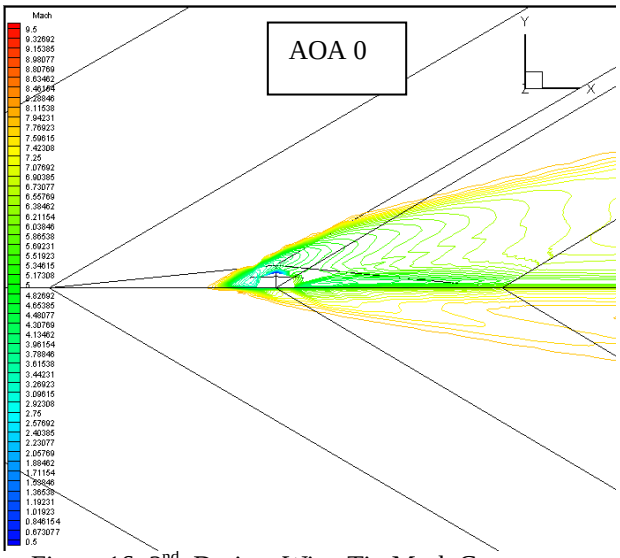


Figure 16: 2nd Design, Wing Tip Mach Contours

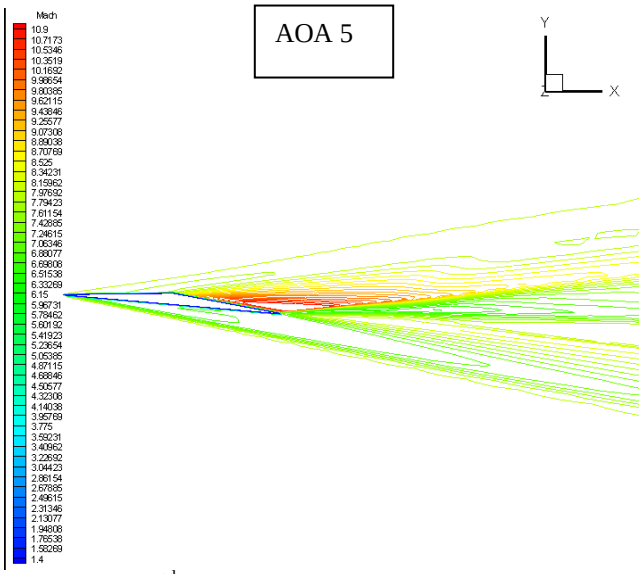


Figure 17: 2nd Design, Center Slice Mach Contours

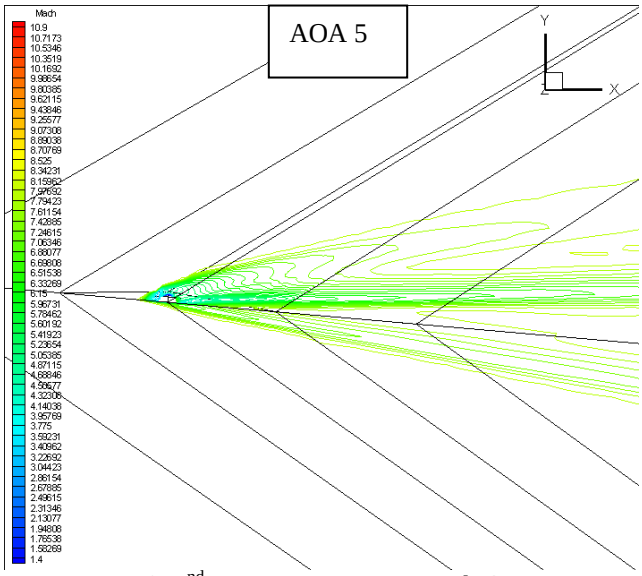


Figure 18: 2nd Design, Wing Tip Mach Contours

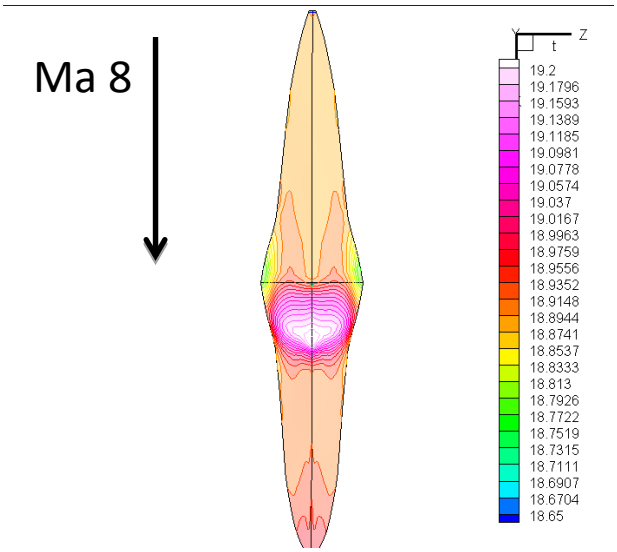


Figure 19: Normalized temperatures, suction side

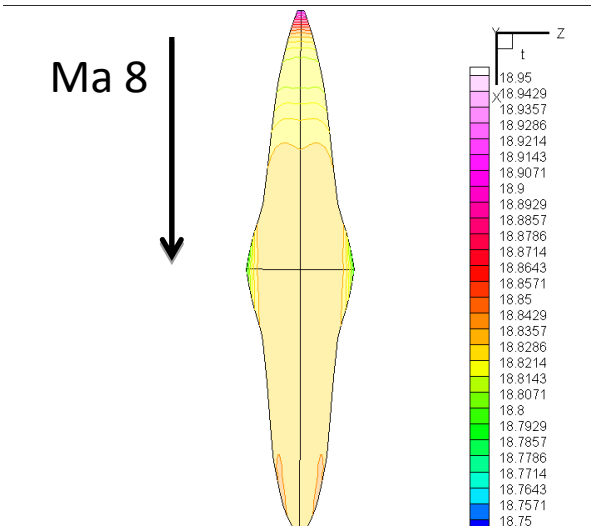


Figure 20: Normalized temperatures, pressure side

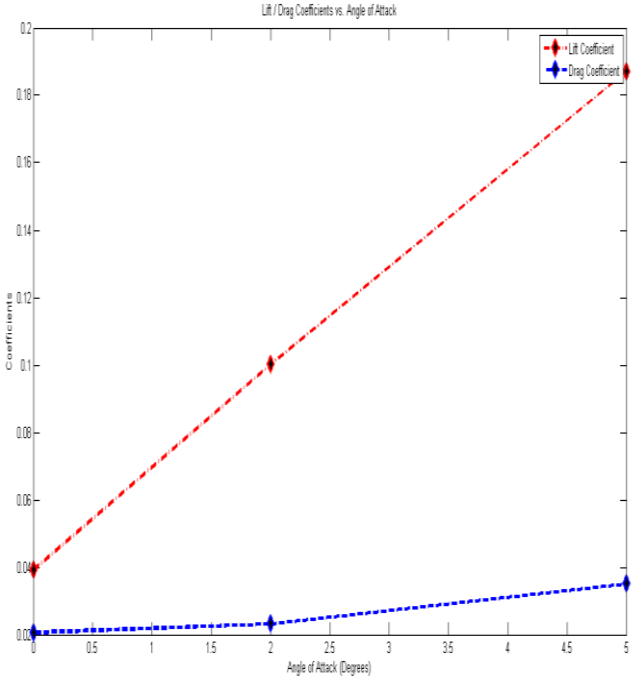


Figure 21: Ma 3, Lift and Drag Coefficients vs. AOA

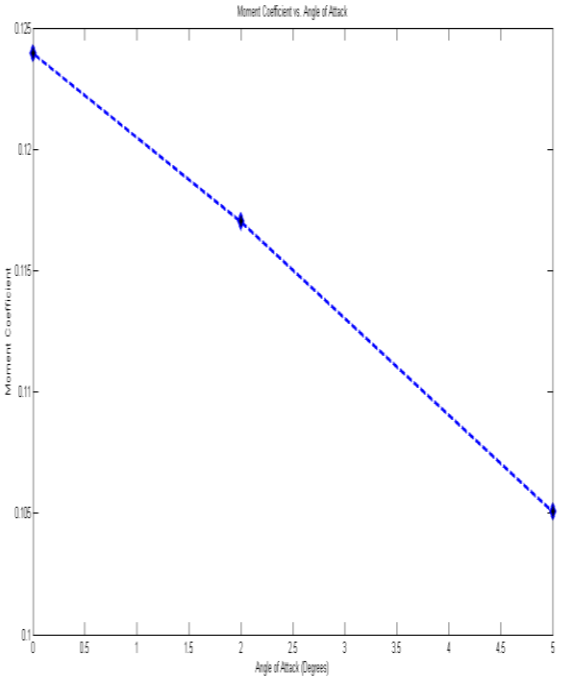


Figure 22: Ma 3, Moment Coefficient vs. AOA

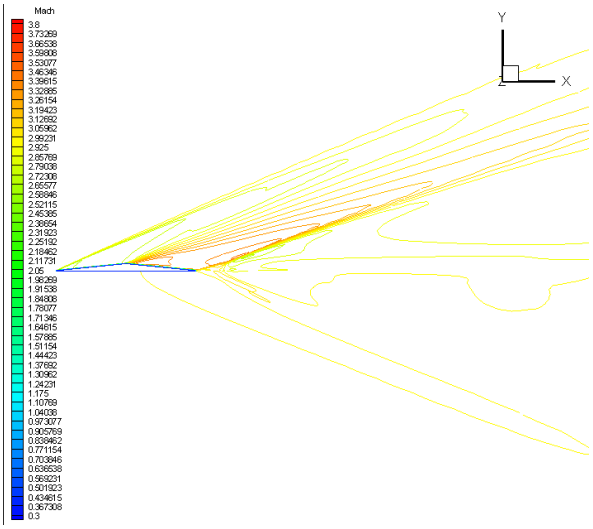


Figure23: Mach 3,Center Slice Mach Contours, AOA0

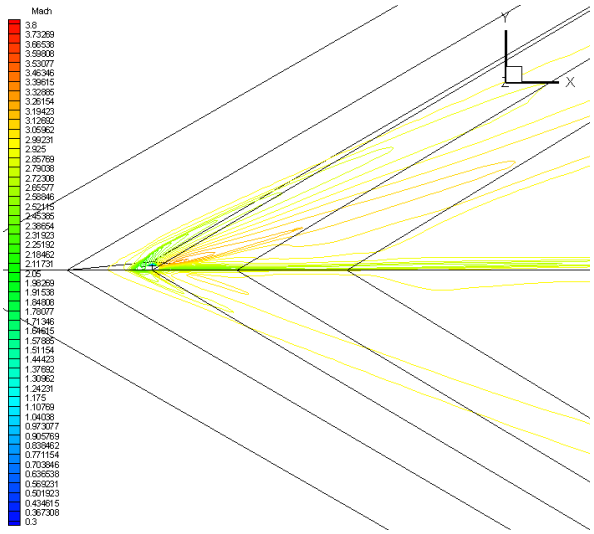


Figure 24: Mach 3,Wing Tip Slice Mach Contours, AOA0

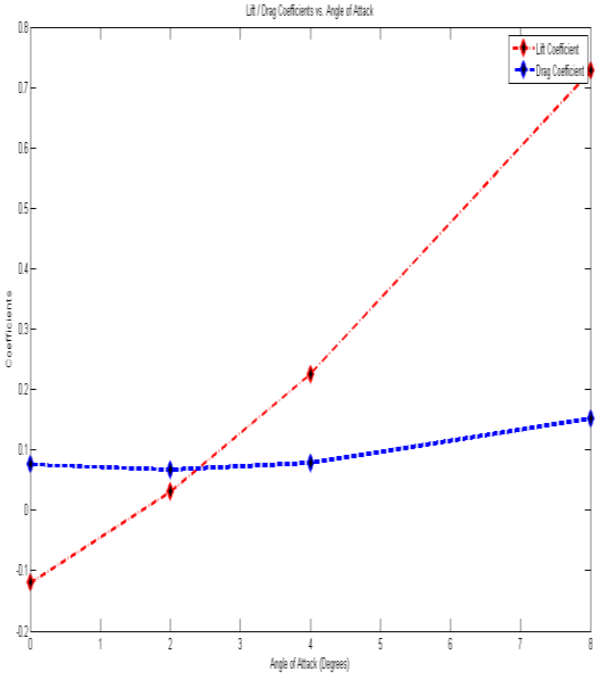


Figure 25: Ma.85, Lift/Drag Coefficient vs. AOA

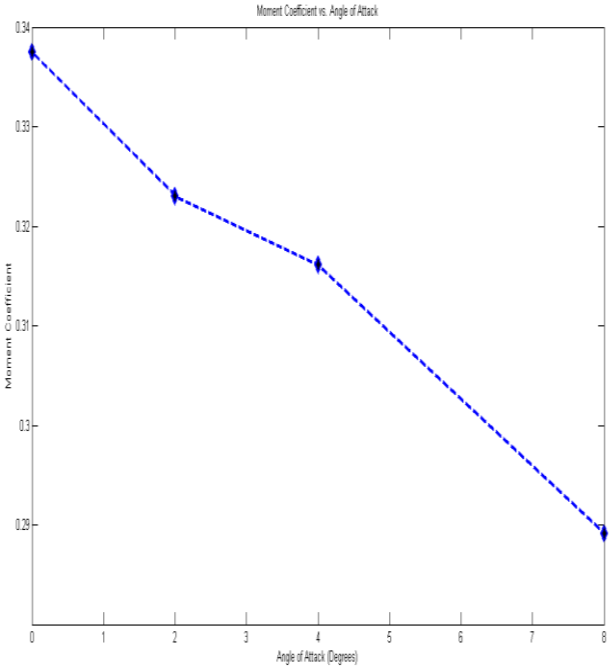


Figure 26: Ma.85, Moment Coefficient vs. AOA

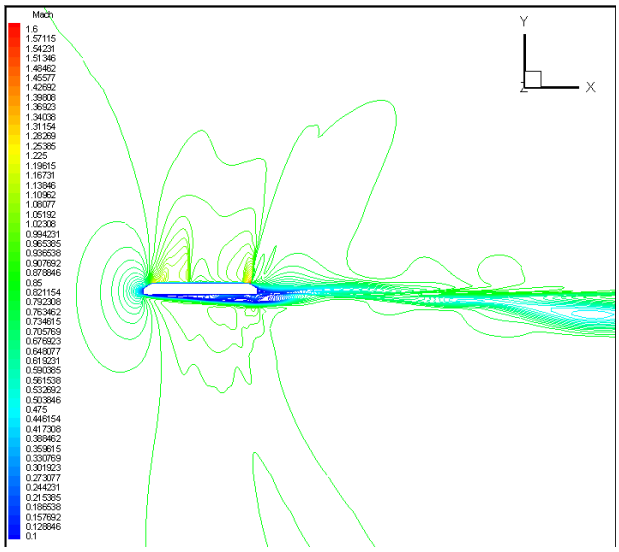


Figure 27: Ma.85, Center Slice Mach Contours, AOA 0

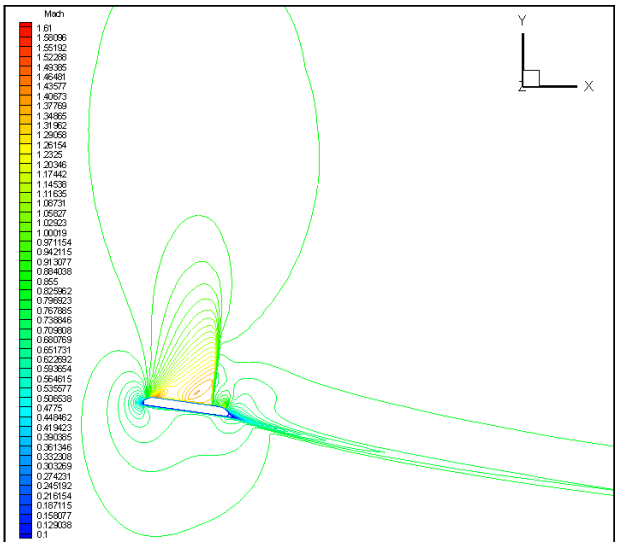


Figure 28: Ma.85, Center Slice Mach Contours, AOA 8

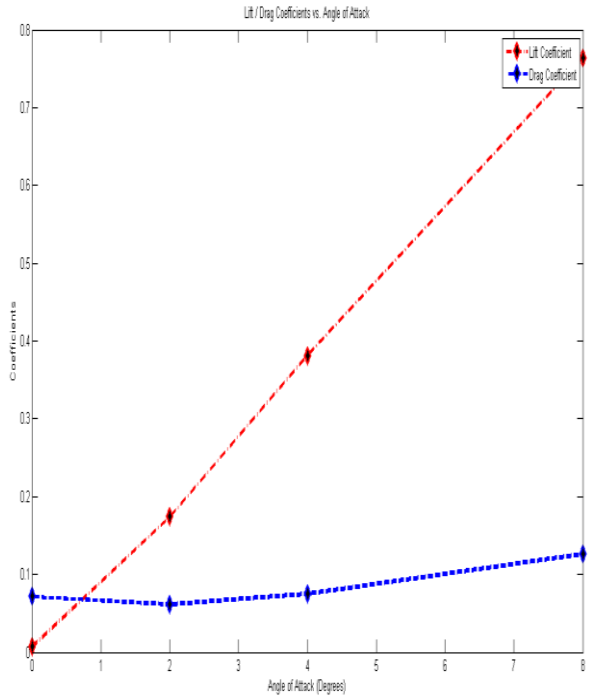


Figure 29: Ma .6, Lift/Drag Coefficient vs. AOA

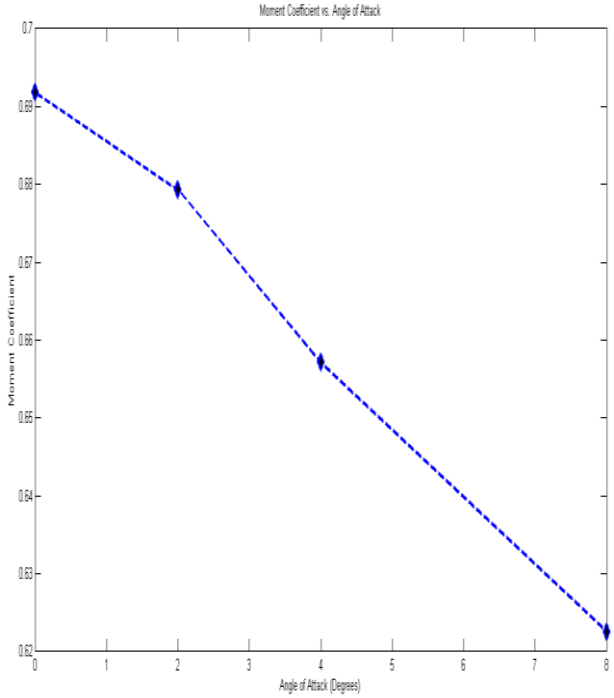


Figure 30: Ma.6, Moment Coefficient vs. AOA

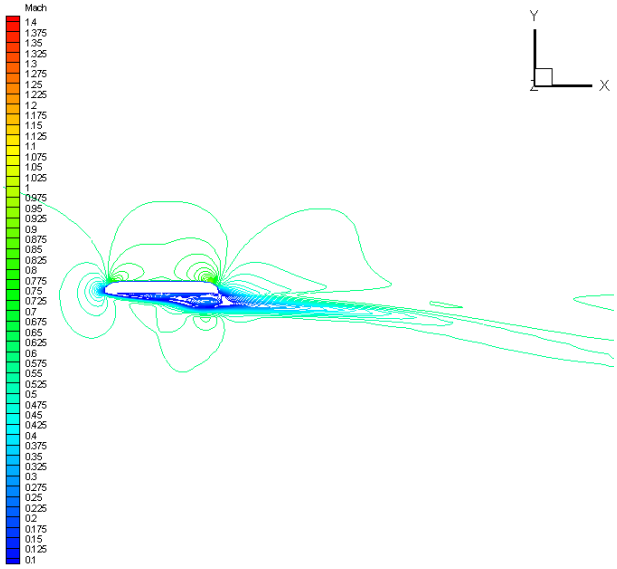


Figure 31: Ma.6,Center Slice Mach Contours, AOA 0

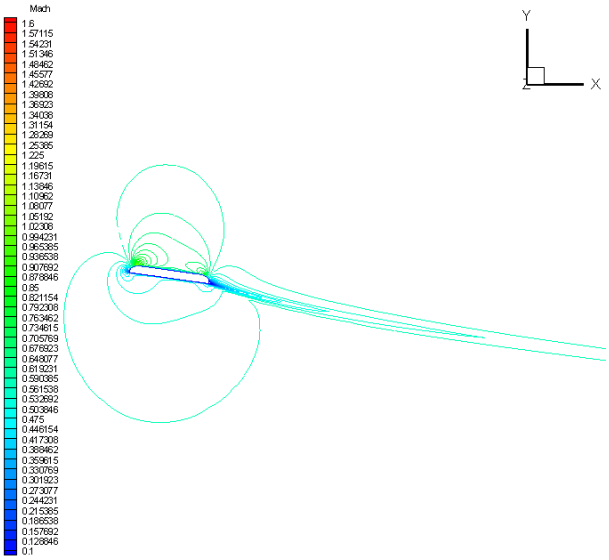


Figure 32: Ma.6, Center Slice Mach Contours, AOA 8

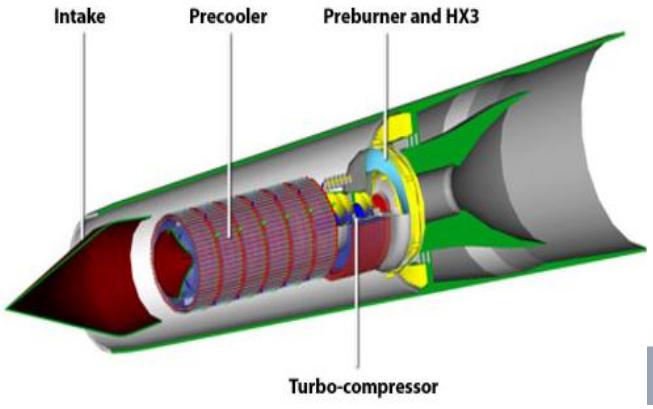


Figure 33:Reactions Engines Scimitar Engine, Ref [10]

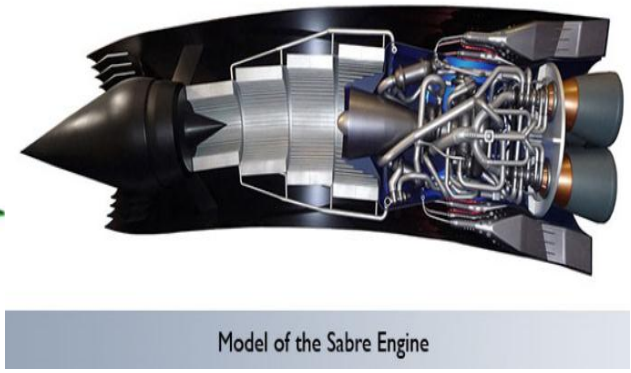


Figure 34:Reactions Engines SABRE Engine Ref [11,12]

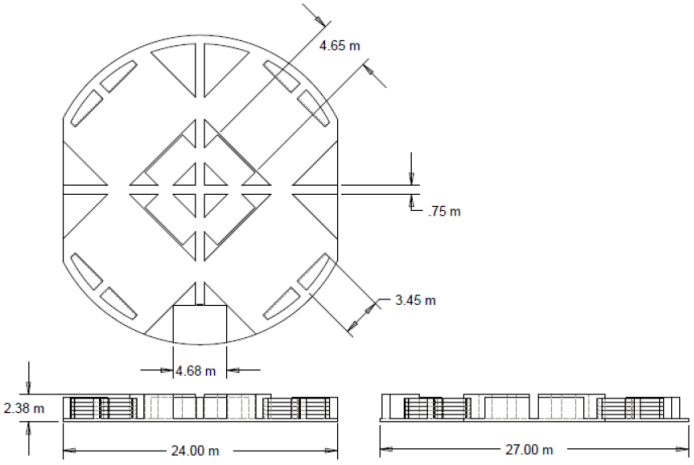


Figure 35: Cabin Floor Layout

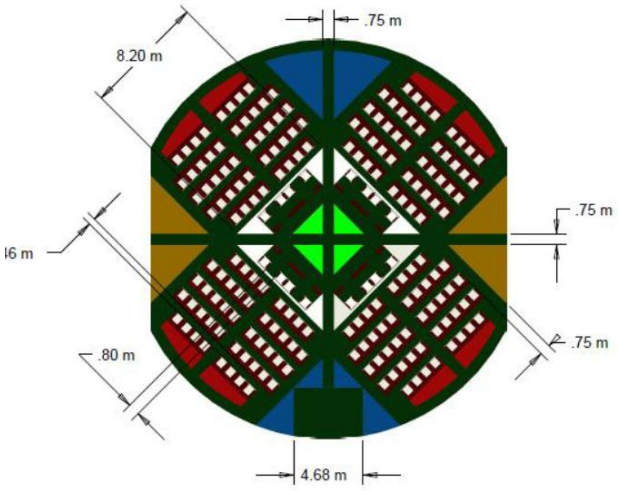


Figure 36: Cabin Floor Plan

## References

[1]Zha, G.-C., Im, H, Espinal, D. "Toward Zero Sonic-Boom and High Efficiency Supersonic Flight, Part I: A Novel Concept of Supersonic Bi-Directional Flying Wing.", AIAA Paper 2010-1013, 48th AIAA Aerospace Sciences Meeting, Orlando, FL, Jan.4-6, 2010.

[2]Espinal, D. and Im, H. and Lee, B. and Sposato, H. and Kinard, D. and Dominguez, J. and Zha, G.-C., " Supersonic Bi-Directional Flying Wing, Part II: Conceptual Design of A High Speed Civil Transport ." AIAA Paper 2010-1393, 48th AIAA Aerospace Sciences Meeting, Orlando, FL, Jan.4-6, 2010.

[3]Zha, G.-C., "Supersonic Flying Wing with Low Sonic Boom, Low Wave Drag, and High Subsonic Performance (SFW-L2HSP)." Technology Transfer Office UMI-163, University of Miami,FL,
Dec. 2008.

[4]Zha, G.-C., "Supersonic Bi-Directional Flying Wing." Provisional patent application No. 61172929, Submitted to USPTO, 27 Apr. 2009.

[5]Zha, G.-C., "Toward Zero Sonic-Boom and High Efficiency Supersonic UAS: A Novel Concept of Supersonic Bi-Directional Flying Wing." US Air Force Academic Outreach UAS Symposium,
Grand Forks, ND, Aug. 4-6, 2009.

[6]Edwards, T. A., "Fluid/Chemistry Modeling for Hypersonic Flight Analysis". *Computers Mathematics Applications.* Vol 24, No. 5/6, 1992.

[7]Bertin, J.J., Cummings, R.M., "Critical Hypersonic Aerothermodynamic Phenomena". Annual Review Fluid Mechanics. Vol 38, 2006.

[8]Milos, F.S., Chen, Y.-K., "Ablation and Thermal Response Property Model Validation for Phenolic Impregnated Carbon Ablator", *Journal of Spacecraft and Rockets.* Vol. 47, No 5, September-October 2010.

[9]Lin, S.-C., Shen, M.-C., “Flight Simulation of a WaveRider-Based Hypersonic Vehicle”.*Computers & Fluids.* Vol. 26, No 1, 1997.

[10]Voland, R.T., Huebner, L.D., McClinton, C.R., “X-43A Hypersonic vehicle technology development”, *Acta Astronautica*. Vol 59, 2006.

[11]Moses, P.L., Rausch, V.L., Nguyen, L.T., Hill, J.R., “NASA hypersonic flight demonstrators – overview,status, and future plans”.*Acta Astronautica.* Vol 55, 2004

[12]Jivraj, F., Varvill, R., Bond, A., Paniagua, G., “The Scimitar Precooled Mach 5 Engine”. 2nd European Conference for Aerospace Sciences.

[13]Murray, J.J., Hempshell, C.M., Bond, A. “An Experimental Precooler for Airbreathing Rocket Engines”. JBIS, Vol 54, 2001.

[14]Varvill, R., Bond, A., “The SKYLON Spaceplane”. JBIS, Vol 57, 2004.

[15]Varvill, R., Bond, A., “A Comparison of Propulsion Concepts for SSTO Reusable Launchers”. JBIS, Vol 56, 2003.

[16]Hirschberg, M., Hart, D. and Beutner, T., “A Summary Of A Half-Century of Oblique Wing Research." AIAA Paper 2007-150, 2007.

[17]Desktop Aeronautics, Inc., “Oblique Flying Wings: An Introduction and White Paper." http://www.desktopaero.com/obliquewing/library/whitepaper/index.html, 2005.

[18]Campbell, J.P., and Drake, H.M., “Investigation of stability and control characteristics of an airplane model with a skewed wing in the Langley free °ight tunnel." NACA TN-1208, May 1947.

[19]Matthews, H. , “Oblique Wing Research Aircraft NASA AD-1." World X-Planes Magazine, No. 2, 2005.

[20]Reithmaier L., Mach 1 and Beyond, The Illustrated Guide to High-Speed Flight. TAB Books, a division of McGraw-Hill, Inc., 1995.

[21]G.-C. Zha, Y. Shen, and B. Wang, “Calculation of Transonic Flows Using WENO Method with a Low Diffusion E-CUSP Upwind Scheme." AIAA Paper 2008-0745, 46th AIAA Aerospace Sciences Meeting, Reno, NV, Jan. 2008.

[22]G.-C. Zha, “Low Diffusion Efficient Upwind Scheme ," AIAA Journal, vol. 43, 2005.

[23]G.-C. Zha and Z.-J. Hu, “Calculation of Transonic Internal Flows Using an Efficient High Resolution Upwind Scheme," AIAA Journal, vol. 42, No. 2, pp. 205-214, 2004.

[24]Shen, Y.-Q. and Zha, G.-C. , “Improvement of the WENO Scheme Smoothness Estimator,"International Journal for Numerical Methods in Fluids, vol. DOI:10.1002/fld.2186, 2009.10

[25]Shen, Y.-Q. and Zha, G.-C. and Chen, X.-Y., “High Order Conservative Differencing for Viscous Terms and the Application to Vortex-Induced Vibration Flows," Journal of Computational Physics, vol. 228(2), pp. 8283{8300, 2009.

[26]Y.-Q. Shen, G.-C. Zha, and B.-Y. Wang, “Improvement of Stability and Accuracy of Implicit WENO Scheme ," AIAA Journal, vol. 47, pp. 331{344, 2009.

[27]Shen, Y.-Q. and Zha, G.-C., “Improved Seventh-Order WENO Scheme ." AIAA Paper 2010-1451, 48th AIAA Aerospace Sciences Meeting, Orlando, FL, Jan. 4-6, 2010.

[28]X. Chen and G.-C. Zha, “Implicit Application of Non-Reflective Boundary Conditions for Navier-Stokes Equations in Generalized Coordinates," International Journal for Numerical Methods in Fluids, vol. 50, 2006.

[29]Z.-J. Hu and G.-C. Zha, “Calculations of 3D Compressible Using an E±cient Low Diffusion Upwind Scheme," International Journal for Numerical Methods in Fluids, vol. 47, pp. 253-269,2004.

[30]Y.-Q. Shen and G.-C. Zha, “A Comparison Study of Gauss-Seidel Iteration Methods for Internal and External Flows ." AIAA Paper 2007-4332, 2007.

[31]X.-Y. Chen, G.-C. Zha, and M.-T. Yang, “Numerical Simulation of 3-D Wing Flutter with Fully Coupled Fluid-Structural Interaction," Journal of Computers & Fluids, vol. 36, No. 5, pp. 856-867, 2007.

[32]X.-Y. Chen and G.-C. Zha, “Fully Coupled Fluid-Structural Interactions Using an Efficient High Resolution Upwind Scheme," Journal of Fluids and Structures, vol. 20, pp. 1105-1125, 2005.

[33]Wang, B. Y and Zha, G.-C., “High Fidelity Simulation of Nonlinear Fluid-Structural Interaction with Transonic Airfoil Limit Cycle Oscillations," Accepted for publication in Journal of Fluids and Structures, 2010.

[34]Wang, B.-Y. and Haddoukessouni, B. and Levy, J. and Zha, G.-C., “Numerical Investigations of Injection Slot Size E®ect on the Performance of Co-Flow Jet Airfoil," Journal of Aircraft, Toappear 2008.

[35]B.Wang and G.-C. Zha, “Comparison of a Low Diffusion E-CUSP and the Roe Scheme for RANS Calculation." AIAA Paper 2008-0596, 46th AIAA Aerospace Sciences Meeting and Exhibit, Jan.7-10, 2008.

[36]Coronado, P. and Wang, B.-Y. and Zha, G.-C., “Delayed-Detached-Eddy Simulation of Shock Wave/Turbulent Boundary Layer Interaction ." AIAA Paper 2010-0109, 48th AIAA Aerospace Sciences Meeting, Orlando, FL, Jan. 4-6, 2010.

[37]Chen, X.-Y. and Wang, B.-Y. and Zha, G.-C. , “Detached Eddy Simulation of 3-D Wing Flutter with Fully Coupled Fluid-Structural Interaction." AIAA Paper 2010-0053, 48th AIAA Aerospace Sciences Meeting, Orlando, FL, Jan. 4-6, 2010.

[38]Y.-Q. Shen and G.-C. Zha, “Comparison of High Order Schemes for Large Eddy Simulation of Circular Cylinder Flow." AIAA-2009-0945, Submitted to Journal of Computational Physics, 2009.

[39]B. Wang and G. - C. Zha , “Detached Eddy Simulations of a Circular Cylinder Using a Low Diffusion E-CUSP and High-Order WENO Scheme." AIAA Paper 2008-3855, AIAA 38th Fluid Dynamics Conference, Seattle, Washington, June 23-26, 2008.

[40]Y.-Q. Shen and G.-C. Zha, “Simulation of Flows at All Speeds with WENO Scheme and Preconditioning." AIAA Paper 2009-1312, AIAA 47th Aerospace Sciences Meeting, Orlando, FL, Jan. 5-8, 2009.

[41]Wang, B.-Y. and Haddoukessouni, B. and Levy, J. and Zha, G.-C., “Numerical Investigations of Injection Slot Size Effect on the Performance of Co-Flow Jet Airfoil ," AIAA Journal of Aircraft, vol. 45, pp. 2084-2091, 2008.

[42]P. Roe, “Approximate Riemann Solvers, Parameter Vectors, and Difference Schemes," Journal of Computational Physics, vol. 43, pp. 357-372, 1981.

[43]B. Van Leer, “Towards the Ultimate Conservative Difference Scheme, III," Journal of Computational Physics, vol. 23, pp. 263-75, 1977.